NUCLEAR INTERACTIONS AND MULTIPLE COULOMB SCATTERING AT VOLUME REFLECTION

M.V. Bondarenco*

National Science Center "Kharkov Institute of Physics and Technology", 61108, Kharkov, Ukraine

(Received November 1, 2011)

For volume reflection of charged particles governed by the continuous potential of atomic planes in a bent crystal, we calculate the probability of a nuclear interaction. It is found to differ from the corresponding probability in an amorphous target by an amount proportional to the crystal bending radius and the particle mean deflection angle, independently of the shape of the interplanar continuous potential. That result is also applied to the description of the final beam angular divergence owing to the multiple Coulomb scattering. The theoretical predictions are compared with the results of recent experiments.

PACS: 61.85.+p, 29.27.-a, 45.10.-b

1. INTRODUCTION

Volume reflection [1] is a phenomenon when a fast charged particle reflects from a family of curved atomic planes of an oriented bent crystal to side opposite to that of the crystal bending. It is considered to be a promising mechanism of local beam steering at high energy particle accelerators. The transverse direction asymmetry in the volume reflection effect originates from the asymmetry of the continuous potential of bent atomic planes, especially in the area where the angles of atomic plane crossing by the particle become comparable to the Lindhard's critical angle $\theta_c = \sqrt{2V_0/E}$, with V_0 the interplanar continuous potential well depth, and $E \gg V_0$ the particle energy. The extent of the volume reflection area is estimated as $\sim R\theta_c$, where R is the crystal bending radius [2].

Although the origin of the volume reflection effect is due to the coherent potential scattering, in a real crystal one must also take into account incoherent Coulomb scattering on individual atomic nuclei at close interactions with them. The condition for the incoherent scattering not to spoil the volume reflection effect is the smallness of the multiple Coulomb scattering r.m.s. angle accumulated along the whole traversed crystal compared to the mean volume reflection angle. That condition permits usage for the volume reflection experiments of the crystals of thickness $1 \div 2$ mm, by ~ 10 times exceeding the essential volume reflection region extent.[1] However, in other respects, for instance for evaluation of the outcoming beam angular divergence, the multiple Coulomb scattering is crucial. Another manifestation of the nuclear interactions at high energy are the multiple hadron production events, which can be registered in downstream detectors (beam loss monitors).

Outside the volume reflection area, the particle motion becomes highly over-barrier and straightens out even relative to the active atomic planes. Thereat, the rate of a fast particle scattering on atomic nuclei must approach that in an amorphous medium (see Sec. 2). In a thick-crystal limit, the number of close nuclear interactions in the whole crystal will be dominated by the pre- and post-volume reflection areas, and will become about equal to that in an amorphous target of same material and thickness. But there remains a finite difference generated in the volume reflection region, which carries information about the volume reflection dynamics and kinetics, and usually is sufficiently sizeable to manifest itself in the experimental data. In the present article we calculate that difference, and compare the result with the recent related measurements. For a more detailed discussion of the involved problems see [3].

2. NUCLEAR INTERACTION PROBABILITY AT VOLUME REFLECTION

The volume reflection implies particle interaction with the bent crystal in a planar orientation. Thereat, the atomic density in each plane may be regarded as uniform. Since all the nuclei are located in the planes, the particle crossing of one atomic plane may be regarded as an elementary act of nuclear interaction. In the simplest case when all the planes are equivalent (which corresponds to silicon crystal in orientation (110)), the surface density of nuclei in each plane equals $n_{\rm at}d$, where $n_{\rm at}$ is the atomic volume density of the crystal, and d the inter-planar dis-

*E-mail address: bon@kipt.kharkov.ua

[1] At an exemplary beam energy $E \simeq 400$ GeV (CERN SPS), which entails $\theta_c \sim 10^{-5}$ rad, and at optimal radius $R \sim 10$ m, this longitudinal scale amounts to $R\theta_c \sim 10^{-1}$ mm.

tance. If nuclear concentrations along the planes may be regarded as thin (despite the thermal broadening) and thus crossed by the fast particle at a definite tangential angle θ, the probability of any kind of nuclear interaction in one atomic plane amounts to

$$P_1 = n_{\rm at}\sigma_A \frac{d}{\sin\theta} \tag{1}$$

with σ_A the corresponding cross-section of the particle interaction with a single nucleus. For elastic scattering one has to take the transport cross-section ($\sigma_A \to \sigma_{\rm tr}$), while for inelastic interactions – the corresponding total inelastic cross-section on a Silicon nucleus ($\sigma_A \to \sigma_{\rm inel}$). Generalization to a case with a few non-equivalent planes within a period (relevant, e.g., for silicon crystal in orientation (111)) is straightforward.

Consider first the case of a straight crystal traversed by a fast particle in a highly over-barrier regime, when the angle θ between the particle momentum and the planes by far exceeds the critical value,

$$\theta \gg \theta_c. \tag{2}$$

Thereat, θ varies negligibly within the crystal ($\mathrm{var}\theta < \theta_c \ll \theta$). Summing up contributions (1) for $\approx \frac{L\sin\theta}{d}$ crossed planes then yields the total nuclear interaction probability:

$$P = P_1 \frac{L\sin\theta}{d} = n_{\rm at}\sigma_A L \quad \text{(highly over-barr. pass.)} \tag{3}$$

This value is independent of d and θ, and equals to the corresponding probability in an amorphous (i.e. polycrystalline) medium – not surprisingly since the uniform particle flow covers each nucleus with the same density, regardless of the existence of a far atomic order in the medium. In that sense, one can as well speak about an "amorphous orientation" of a perfect crystal.

Next we consider the case of a bent crystal, to which a particle enters and exits in a highly over-barrier regime, but undergoes volume reflection somewhere in the middle of the crystal. In the vicinity of the reflection point, the particle transverse kinetic energy is comparable to the potential energy, and condition (2) breaks down, and the "amorphous orientation" does not apply. Thereat, the plane crossing angle varies considerably along the particle path, and from plane to plane. Hence, for accurate evaluation of nuclear interaction probabilities (1) at each plane crossing, one needs at least to evaluate the whole trajectory beyond the straight line approximation. Within the volume reflection region, it may be legitimate to neglect the multiple Coulomb scattering entirely, and compute the particle trajectory in the pure continuous potential. That will be our approximation in the present article.

Provided the crystal is bent uniformly (which is sufficiently credible at present technology level), the trajectory description simplifies in cylindrical coordinates, with the bent planes corresponding to surfaces of constant radius relative to some axis far outside the crystal. Thereat, the plane crossing angle sine entering Eq. (1) expresses simply as the time derivative of the particle radial coordinate:

$$\sin\theta \approx \dot{r}/c \tag{4}$$

(we deal with ultra-relativistic particles moving nearly at speed of light c). Inserting (4) to Eq. (1) and summing over all the planes crossed by the particle, we obtain the total inelastic nuclear interaction probability in a bent crystal:

$$P \approx n_{\rm at}\sigma_A cd \sum_n \frac{1}{\dot{r}_n} \qquad \text{(unif. bent crystal)}. \tag{5}$$

Since the particle motion is supposed to straighten out away from the volume reflection area, there the nuclear interaction rate per unit length must approach that in an amorphous medium. Hence, the difference between the number of nuclear interactions in an oriented crystal and in an "unoriented" crystal may be expressed as

$$\Delta P = n_{\rm at}\sigma_A \Delta L \tag{6}$$

with the isolated geometrical factor

$$\Delta L = \lim_{L\to\infty}\left(\sum_n \frac{cd}{\dot{r}_n} - L\right), \tag{7}$$

expected to be finite and independent of L, representing the excess (or deficit) of the target nuclear interaction range.

The evaluation of limit (7) and averaging over the angles and impact parameters of particles in the initial beam simplifies under the condition $R \gg R_c$, and may be performed without the need to specify the exact shape of the inter-planar potential. For positively charged particles, the result reads [3]:

$$\langle\Delta L\rangle = R\,\langle\chi\rangle\left(1 + \mathcal{O}(R_c^2/R^2)\right) \qquad \text{(pos. particles)}, \tag{8}$$

where $\langle\chi\rangle$ is the correspondingly averaged deflection angle of particles in the crystal. Importantly, $\langle\chi\rangle$ includes $\mathcal{O}(R_c/R)$ corrections (cf. Eq. (17) below), which may be important at practice, but higher order corrections are beyond the accuracy of relation (8). Remarkably, result (8) holds both in orientations (110) and (111).

For negatively charged particles, at leading order in R_c/R, when $\langle\chi\rangle \approx \theta_c$, the result is similar to (8):

$$\langle\Delta L\rangle = -R\theta_c\,(1 + \mathcal{O}(R_c/R)) \qquad \text{(neg. particles)}. \tag{9}$$

Corrections $\mathcal{O}(R_c/R)$ can also be computed, but they are not absorbable into $\langle\chi\rangle$ and differ for (110) and (111) orientations (see [3]).

The principal difference between Eq. (8) and (9) is that for positive particles the nuclear range excess is positive, while for negative particles it is negative (representing a deficit), being of the same order in magnitude. That property is natural from

the viewpoint that positive particles are repelled from the atomic planes and cross them more tangentially, while negative particles are attracted, crossing the planes quicker.

3. COMPARISON WITH THE EXPERIMENTAL DATA

Inelastic nuclear interaction probability. Predictions (8, 9) can be tested against the available experimental data. The most direct check is supposed to be against the results of experiments on inelastic nuclear scattering. At present, there is one such experiment, performed at CERN with 400 GeV protons and a $L = 2$ mm thick silicon crystal at a single value of the crystal bending radius $R = 10$ m [4].

When the cutting angle (essentially the initial beam collimation angle) was sufficiently large (which ought to correspond to perfect averaging over b or $E_\perp$), the measured relative difference between the number of inelastic nuclear interaction events at volume reflection and in the "amorphous orientation" was about constant, holding on the level

$$\frac{\Delta P}{P} \approx (5 \pm 2)\%. \qquad \text{(experim.)} \tag{10}$$

For comparison, our prediction, using the experimentally determined [7] mean value $\langle\chi\rangle_{\rm exp} = 13.35\,\mu$rad at the given curvature $1/R = 0.1\,\mathrm{m}^{-1}$ amounts to

$$\frac{\Delta P}{P} = \frac{\langle\Delta L\rangle}{L} = \frac{R\,\langle\chi\rangle_{\rm exp}}{L} = 6.67\%. \qquad \text{(theor.)} \tag{11}$$

The agreement between (10) and (11) may be regarded as satisfactory.

Impact on the final beam angular divergence. The nuclear interactions also manifest themselves through angular broadening of the final beam due to elastic Coulomb scattering. There is, however, another contribution to the broadening, present even in a pure continuous potential, and stemming from the impact parameter dependence of the deflection angle. In fact, the continuous potential contribution is absent in the direction parallel to the planes, but the beam spread parallel to the planes is rarely measured, so in the published experimental data on the beam dispersion in the direction of deflection the amorphous and continuous potential contributions enter together.

Reasonably, we can decompose the kinetics of the particle passage through the crystal into three distinct stages: pure incoherent multiple scattering upstream the volume reflection region (where the beam acquires Gaussian shape), pure dynamical broadening in the volume reflection region, and pure incoherent multiple scattering downstream of it. Denoting by $dw/d\chi$ the final angular distribution function, and by $dw_{\rm coh}/d\chi$ the intrinsic volume reflection distribution function, obtained with the neglect of multiple Coulomb scattering, the aggregate angular dispersion

$$\sigma^2 = \int_{-\infty}^{\infty} d\chi\,(\chi - \langle\chi\rangle)^2\,\frac{dw}{d\chi} \qquad \left(\int_{-\infty}^{\infty} d\chi \frac{dw}{d\chi} = 1\right) \tag{12}$$

about the mean value

$$\langle\chi\rangle = \int_{-\infty}^{\infty} d\chi\chi\frac{dw}{d\chi} \tag{13}$$

is represented as a sum of independent contributions:

$$\begin{aligned}\sigma^2 &= \sigma^2_{\rm am}(L + \langle\Delta L\rangle) + \sigma^2_{\rm coh} \\ &\equiv \sigma^2_{\rm am}(L) + \sigma^2_{\rm am}(R\,\langle\chi\rangle) + \sigma^2_{\rm coh},\end{aligned} \tag{14}$$

with

$$\sigma^2_{\rm coh} = \int_{-\infty}^{\infty} d\chi\,(\chi - \langle\chi\rangle)^2\,\frac{dw_{\rm coh}}{d\chi}, \tag{15}$$

and provided $\sigma^2_{\rm am}(T)$ is a linear function of T (see Eq. (19) below).

The intrinsic angular distribution $dw_{\rm coh}/d\chi$ was evaluated in [5] in the model of harmonic continuous potential between (110) silicon crystallographic planes. It has some differences for positive and negative particles, as does the nuclear interaction rate described in Sec. 2.

Positively charged particles. For positive particles, at $R > 4R_c$ the angular distribution of the intrinsic volume reflection has approximately rectangular shape (see Eq. (72) of [5], where the calculation was conducted in the harmonic approximation for the interplanar continuous potential)[2]

$$\frac{dw_{\rm coh}}{d\chi} \approx \frac{R\theta_c}{\pi d}\Theta\left(\frac{\pi d}{2R\theta_c} - |\chi - \langle\chi\rangle|\right). \tag{16}$$

In Eq. (16) $\Theta(s)$ is the Heavyside unit step function, and $\langle\chi\rangle$ equals[3]

$$\langle\chi\rangle \approx \theta_{\rm lim}\left(1 - \frac{d}{\theta_c^2 R}\right), \qquad \theta_{\rm lim} = \frac{\pi}{2}\theta_c. \tag{17}$$

By Eq. (15), the corresponding $\sigma_{\rm coh}$ is found to be

$$\sigma_{\rm coh} \approx \frac{\pi}{2\sqrt{3}\theta_c}\frac{d}{R}, \tag{18}$$

notably being inversely proportional to the crystal bending radius.

For $\sigma_{\rm am}$ we may adopt the simple formula of Gaussian diffusion:

$$\sigma_{\rm am}(T) \approx \frac{E_0}{E}\sqrt{\frac{T}{X_0}}, \tag{19}$$

with X_0 the radiation length ($X_0 \approx 9.36\,$cm for silicon), and E_0 an universal constant. With the account of Rutherford asymptotics of the scattering cross-section, and of the distribution function at large

[2] In paper [5] the final beam angular distribution was described in terms of $d\lambda/d\chi$, the differential cross-section. But obviously, dividing that quantity by d, we obtain the normalized probability distribution $\frac{dw_{\rm coh}}{d\chi} = \frac{1}{d}\frac{d\lambda}{d\chi}$, $\int d\chi \frac{dw_{\rm coh}}{d\chi} = 1$ handled in the present paper.

[3] Note that $d/\theta_c^2 \approx 2R_c$, but when the continuous potential is not exactly harmonic, expression d/θ_c^2 works better.

χ, σ^2 defined by Eq. (12) logarithmically diverges, but instead it can be determined from a Gaussian fit to the experimentally measured distribution [9]. In this case, E_0 weakly depends on T, and in the range $T \sim 0.2 \div 1$ mm, practically important for volume reflection, the approximate value for E_0 is $E_0 \approx 11$ MeV (see [3]).

Measurements of total σ^2 for 400 GeV protons interacting with a (110) silicon crystal were made in CERN experiment [7]. There, in order to get access to the intrinsic volume reflection angular divergence $\sigma_{\rm coh}$, the difference

$$\sigma^2 - \sigma^2_{\rm am}(L) = \bar{\sigma}^2_{\rm v.r.} \qquad (20)$$

was evaluated. Yet, according to Eq. (14), it differs from pure $\sigma_{\rm coh}$:

$$\bar{\sigma}_{\rm v.r.} = \sqrt{\sigma^2 - \sigma^2_{\rm am}} = \sqrt{\sigma^2_{\rm coh} + \sigma^2_{\rm am}(R\,\langle\chi\rangle)}. \qquad (21)$$

Inserting explicit theoretical expressions (18), (19) into Eq. (21) leads to a non-scaling dependence of the measured quantity $\bar{\sigma}_{\rm v.r.}$ on R:

$$\bar{\sigma}_{\rm v.r.} = \sqrt{\frac{\pi^2}{12\theta_c^2}\frac{d^2}{R^2} + \frac{\pi\theta_c}{2}\left(\frac{E_0}{E}\right)^2 \frac{R - d/\theta_c^2}{X_0}}. \qquad (22)$$

The most characteristic feature of function (22) is the existence of a minimum with respect to variation of R. The minimum location is found by differentiating the radicand:

$$R_*(E) = \frac{1}{\theta_c}\sqrt[3]{\frac{\pi}{3}X_0 d^2}\left(\frac{E}{E_0}\right)^{2/3} \simeq \left(\frac{E}{38\,\text{GeV}}\right)^{7/6} \text{[m]}. \qquad (23)$$

It may serve to mark the scale of R where the multiple scattering compares with coherent deflection angles.

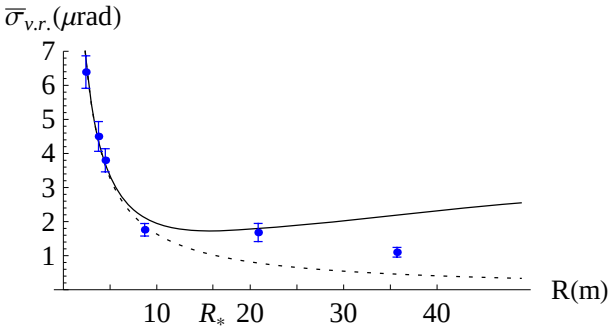

Subtracted final beam angular width vs. the crystal bending radius, for $E = 400$ GeV protons in a $L = 2$ mm silicon crystal. Solid curve: theoretical prediction [Eq. (22)]. Dotted curve: pure $\sigma_{\rm coh}$ (also compatible with calculation of [10] in a more realistic continuous potential model). Points: experimental data [7]

The data of experiment [7] do show a flattening of the R-dependence around R_* (see the figure), but at greater R there is an indication of further decrease. More experimental points in the region $R > R_*$ are needed to establish a clear trend.

Negatively charged particles. For negative particles the experimental data are yet too scarce to extract a picture of $\bar{\sigma}^2_{\rm v.r.}(R)$ behavior, so we restrict ourselves to a few remarks.

For negatively charged particles the expression for $\sigma_{\rm coh}(R)$ differs only by a numerical coefficient (actually, logarithmically dependent on R), but the main $\sim 1/R$-dependence remains. But according to Eq. (4), the difference of the amorphous contribution changes sign: $\Delta\sigma^2_{\rm am} \propto \langle\Delta L\rangle < 0$. Therefore, the expression for $\bar{\sigma}^2_{\rm v.r.}$ for negative particles is similar to the radicand of Eq. (22), but with a negative coefficient at the second term. That implies that for negative particles $\bar{\sigma}^2_{\rm v.r.}$ turns to zero at some value of R, and becomes *negative* beyond it. That is the salient feature of the final beam angular distribution for negative particles, which would be interesting to verify experimentally.

Secondly, since $\sigma_{\rm coh}$ for positively and for negatively charged particles differ, in general it is not as straightforward to compare the angular broadenings for positive and negative particles, as it was for the rate of inelastic nuclear interactions. However, in the region $R > R_c$ where $\sigma_{\rm coh}$ gets relatively small, that must become possible. The simplest way of pinning down $\sigma_{\rm coh}$, though, is to measure both angular beam divergence components perpendicular and parallel to the family of the active atomic planes.

Acknowledgement

The author thanks to V. Guidi and A.V. Shchagin for discussions and to A.M. Taratin for useful correspondence.

References

1. A.M. Taratin and S.A. Vorobiev. Deflection of high-energy charged particles in quasi-channeling states in bent crystals // *Nucl. Instrum. Methods.* 1987, v. B26, p. 512-521;
A.G. Afonin et al. The schemes of proton extraction from IHEP accelerator using bent crystals // *Nucl. Instrum. Methods.* 2005, v. B234, p. 14-22;
V.M. Biryukov et al. Crystal collimation as an option for the large hadron colliders // *Nucl. Instrum. Methods.* 2005, v. B234, p. 23-30;
V. Shiltsev et al. Channeling and volume reflection based crystal collimation of tevatron circulating beam halo (T-980) // *Proc. of IPAC-2010*, Kyoto, Japan, p. 1243-1245.

2. A.M. Taratin and W. Scandale. Volume reflection of high-energy protons in short bent crystals // *Nucl. Instrum. Methods.* 2007, v. B262, p. 340-347.

3. M.V. Bondarenco. Account of Nuclear Scattering at Volume Reflection // *arXiv*: 1108.0648v1.

4. W. Scandale et al. Probability of inelastic nuclear interactions of high-energy protons in a bent

crystal // *Nucl. Instrum. Methods.* 2010, v. B268, p. 2655-2659.

5. M.V. Bondarenco. Model solution for volume reflection of relativistic particles in a bent crystal // *Phys. Rev.* 2010, v. A82, 042902, 19 p.

6. M.V. Bondarenco. Comments on theory of volume reflection and radiation in bent crystals // *Il Nuov. Cim.* 2011, v. C34, p. 381-388.; *arXiv*: 1103.0770.

7. W. Scandale et al. Volume Reflection Dependence of 400 GeV/c Protons on the Bent Crystal Curvature // *Phys. Rev. Lett.* 2008, v. 101, 234801, 4 p.

8. W. Scandale et al. Observation of channeling and volume reflection in bent crystals for high-energy negative particles // *Phys. Lett.* 2009, v. B681, p. 233–236.

9. G.R. Lynch and O.I. Dahl // *Nucl. Instrum. Methods.* 1991, v. B58, p. 6;
V.L. Highland // *Nucl. Instr. Methods.* 1975, v. 129, p. 497; *ibid.* 1979, v. 161, p. 171;
K. Nakamura et al. (Particle Data Group) // *Review of Particle Physics. J. Phys.* 2010, v. G37, 075021.

10. V.A. Maisheev. Volume reflection of ultrarelativistic particles in single crystals // *Phys. Rev. ST Accel. Beams.* 2007, v. 10, 084701, 11 p.

11. Yu.A. Chesnokov et al. Radiation of photons in process of charge particle volume reflection in bent single crystal // *JINST.* 2008, v. 3, P020052;
A.G. Afonin et al. Investigation of the emission of photons induced in the volume reflection of 10-GeV positrons in a bent silicon single crystal // *JETP Lett.* 2008, v. 88, p. 414-417;
W. Scandale et al. Experimental study of the radiation emitted by 180-GeV/c electrons and positrons volume-reflected in a bent crystal // *Phys. Rev.* 2009, v. A79, 012903, 9 p.;
M.V. Bondarenco. Coherent bremsstrahlung in a bent crystal // *Phys. Rev.* 2010, v. A81, 052903, 14 p.;
Yu.A. Chesnokov et al. Photoproduction of electron-positron pairs in bent single crystals // *Phys. Rev. ST Accel. Beams.* 2010, v. 13, 070706, 6 p.

12. V. Biryukov. The Theory of the scattering induced feeding in in bent crystals // *Phys. Lett.* 1995, v. A205, p. 340-343;
V.M. Biryukov and S. Bellucci. Simulations of volume reflection and capture in bent crystals // *Nucl. Instr. Methods.* 2008, v. B266, p. 235-241;
V.M. Biryukov. The Limits of volume reflection in bent crystals // *Nucl. Instr. Methods.* 2009, v. B26, p. 2457-2459.

ЯДЕРНЫЕ ВЗАИМОДЕЙСТВИЯ И МНОГОКРАТНОЕ КУЛОНОВСКОЕ РАССЕЯНИЕ ПРИ ОБЪЕМНОМ ОТРАЖЕНИИ

Н.В. Бондаренко

Для объемного отражения заряженных частиц, управляемого непрерывным потенциалом атомных плоскостей в изогнутом кристалле, мы вычисляем вероятность ядерного взаимодействия. Найдено, что последняя отличается от соответствующей величины в аморфной мишени на величину, пропорциональную радиусу изгиба кристалла и среднему углу отклонения частиц, независимо от конкретной формы межплоскостного непрерывного потенциала. Данный результат также применяется для описания угловой расходимости, приобретенной пучком за счет многократного кулоновского рассеяния в мишени. Теоретические предсказания сравниваются с результатами недавних экспериментов.

ЯДЕРНІ ЗІТКНЕННЯ ТА БАГАТОРАЗОВЕ КУЛОНІВСЬКЕ РОЗСІЯННЯ ПРИ ОБ'ЄМНОМУ ВІДБИТТІ

М.В. Бондаренко

Для об'ємного відбиття заряджених частинок, зумовленого неперервним потенціалом атомних площин в зігнутому кристалі, ми обчислюємо вірогідність ядерного зіткнення. Знайдено, що остання відрізняється від відповідної величини в аморфній мішені на величину, пропорційну радіусу згину кристалу та середньому куту відхилення частинок, незалежно від конкретної форми міжплощинного неперервного потенціалу. Даний результат також застосовується для опису кутового розходження набутого пучком за рахунок багаторазового кулонівського розсіяння в мішені. Теоретичні передбачення порівнюються з результатами недавніх експериментів.